Search for CP Violation in $\tau^{\pm} \to K_S^0 \pi^{\pm} \nu_\tau$ Decays at Belle

M. Bischofberger,[26] H. Hayashii,[26] K. Adamczyk,[29] H. Aihara,[44] V. Aulchenko,[1,33] A. M. Bakich,[39] V. Balagura,[13] E. Barberio,[24] K. Belous,[12] A. Bozek,[29] M. Bračko,[22,14] T. E. Browder,[7] P. Chen,[28] B. G. Cheon,[50] C.-C. Chiang,[28] I.-S. Cho,[49] K. Cho,[17] Y. Choi,[38] M. Danilov,[13] Z. Doležal,[2] A. Drutskoy,[4] S. Eidelman,[1,33] D. Epifanov,[1,33] B. Golob,[21,14] H. Ha,[18] J. Haba,[51] K. Hayasaka,[25] Y. Horii,[43] Y. Hoshi,[42] W.-S. Hou,[28] Y. B. Hsiung,[28] H. J. Hyun,[19] K. Inami,[25] A. Ishikawa,[35] R. Itoh,[51] M. Iwabuchi,[49] Y. Iwasaki,[51] T. Julius,[24] J. H. Kang,[49] H. Kawai,[3] T. Kawasaki,[31] C. Kiesling,[23] H. O. Kim,[19] M. J. Kim,[19] Y. J. Kim,[6] K. Kinoshita,[4] B. R. Ko,[18] P. Kodyš,[2] P. Križan,[21,14] Y.-J. Kwon,[49] S.-H. Kyeong,[49] J. S. Lange,[5] M. J. Lee,[37] S.-H. Lee,[18] J. Li,[7] Y. Li,[47] C. Liu,[36] R. Louvot,[20] J. MacNaughton,[51] S. McOnie,[39] K. Miyabayashi,[26] H. Miyata,[31] Y. Miyazaki,[25] R. Mizuk,[13] G. B. Mohanty,[40] A. Moll,[23,41] T. Mori,[25] Y. Nagasaka,[8] E. Nakano,[34] M. Nakao,[51] H. Nakazawa,[52] S. Nishida,[51] K. Nishimura,[7] O. Nitoh,[46] T. Ohshima,[25] S. Okuno,[15] G. Pakhlova,[13] H. Park,[19] H. K. Park,[19] M. Petrič,[14] L. E. Piilonen,[47] M. Röhrken,[16] S. Ryu,[37] H. Sahoo,[7] Y. Sakai,[51] O. Schneider,[20] C. Schwanda,[11] K. Senyo,[25] M. Shapkin,[12] J.-G. Shiu,[28] B. Shwartz,[1,33] F. Simon,[23,41] P. Smerkol,[14] Y.-S. Sohn,[49] S. Stanič,[32] M. Starič,[14] T. Sumiyoshi,[45] Y. Teramoto,[34] K. Trabelsi,[51] S. Uehara,[51] T. Uglov,[13] S. Uno,[51] G. Varner,[7] A. Vinokurova,[1,33] A. Vossen,[9] C. H. Wang,[27] P. Wang,[10] M. Watanabe,[31] Y. Watanabe,[15] E. Won,[18] H. Yamamoto,[43] Y. Yamashita,[30] C. Z. Yuan,[10] P. Zhou,[48] V. Zhulanov,[1,33] and T. Zivko[14]

(Belle Collaboration)

[1]*Budker Institute of Nuclear Physics, Novosibirsk*
[2]*Faculty of Mathematics and Physics, Charles University, Prague*
[3]*Chiba University, Chiba*
[4]*University of Cincinnati, Cincinnati, Ohio 45221*
[5]*Justus-Liebig-Universität Gießen, Gießen*
[6]*The Graduate University for Advanced Studies, Hayama*
[7]*University of Hawaii, Honolulu, Hawaii 96822*
[8]*Hiroshima Institute of Technology, Hiroshima*
[9]*University of Illinois at Urbana-Champaign, Urbana, Illinois 61801*
[10]*Institute of High Energy Physics, Chinese Academy of Sciences, Beijing*
[11]*Institute of High Energy Physics, Vienna*
[12]*Institute of High Energy Physics, Protvino*
[13]*Institute for Theoretical and Experimental Physics, Moscow*
[14]*J. Stefan Institute, Ljubljana*
[15]*Kanagawa University, Yokohama*
[16]*Institut für Experimentelle Kernphysik, Karlsruher Institut für Technologie, Karlsruhe*
[17]*Korea Institute of Science and Technology Information, Daejeon*
[18]*Korea University, Seoul*
[19]*Kyungpook National University, Taegu*
[20]*École Polytechnique Fédérale de Lausanne (EPFL), Lausanne*
[21]*Faculty of Mathematics and Physics, University of Ljubljana, Ljubljana*
[22]*University of Maribor, Maribor*
[23]*Max-Planck-Institut für Physik, München*
[24]*University of Melbourne, School of Physics, Victoria 3010*
[25]*Nagoya University, Nagoya*
[26]*Nara Women's University, Nara*
[27]*National United University, Miao Li*
[28]*Department of Physics, National Taiwan University, Taipei*
[29]*H. Niewodniczanski Institute of Nuclear Physics, Krakow*
[30]*Nippon Dental University, Niigata*
[31]*Niigata University, Niigata*
[32]*University of Nova Gorica, Nova Gorica*
[33]*Novosibirsk State University, Novosibirsk*
[34]*Osaka City University, Osaka*
[35]*Saga University, Saga*
[36]*University of Science and Technology of China, Hefei*
[37]*Seoul National University, Seoul*

[38]Sungkyunkwan University, Suwon
[39]School of Physics, University of Sydney, NSW 2006
[40]Tata Institute of Fundamental Research, Mumbai
[41]Excellence Cluster Universe, Technische Universität München, Garching
[42]Tohoku Gakuin University, Tagajo
[43]Tohoku University, Sendai
[44]Department of Physics, University of Tokyo, Tokyo
[45]Tokyo Metropolitan University, Tokyo
[46]Tokyo University of Agriculture and Technology, Tokyo
[47]CNP, Virginia Polytechnic Institute and State University, Blacksburg, Virginia 24061
[48]Wayne State University, Detroit, Michigan 48202
[49]Yonsei University, Seoul
[50]Hanyang University, Seoul
[51]High Energy Accelerator Research Organization (KEK), Tsukuba
[52]National Central University, Chung-li
(Received 1 January 2011; published 23 September 2011)

We report on a search for CP violation in $\tau^\pm \to K_S^0\pi^\pm\nu_\tau$ decays using a data sample of 699 fb^{-1} collected by the Belle experiment at the KEKB electron-positron asymmetric-energy collider. The CP asymmetry is measured in four bins of the invariant mass of the $K_S^0\pi^\pm$ system and found to be compatible with zero with a precision of $O(10^{-3})$ in each mass bin. Limits for the CP violation parameter $\mathrm{Im}(\eta_S)$ are given at the 90% confidence level. These limits are $|\mathrm{Im}(\eta_S)| < 0.026$ or better, depending on the parametrization used to describe the hadronic form factors, and improve upon previous limits by 1 order of magnitude.

DOI: 10.1103/PhysRevLett.107.131801 PACS numbers: 13.35.Dx, 11.30.Er, 12.60.Fr, 14.80.Fd

To date CP violation (CPV) has been observed only in the K and B meson systems. In the standard model (SM), all observed CPV effects can be explained by the irreducible complex phase in the Cabibbo-Kobayashi-Maskawa quark mixing matrix [1]. To find new physics, it is important to look for other CP-violating effects in as many systems as possible. One such system is the τ lepton. In hadronic τ decays, one can search for CPV effects of possible new physics that could originate, for example, from the minimal supersymmetric standard model [2,3] or from multi-Higgs-doublet models (MHDM) [4,5] that play an important role in strangeness changing processes.

This Letter describes a search for CPV in $\tau^\pm \to K_S^0\pi^\pm\nu_\tau$ decays. It should be noted that CPV in K^0 decays leads to a small SM CP asymmetry of $O(10^{-3})$ in the rates of this τ decay mode [6,7]. This asymmetry is just below our experimental sensitivity. Here the focus will be on CPV that could arise from a charged scalar boson exchange [8], e.g., a charged Higgs boson. This type of CPV cannot be observed from measurement of $\tau^\pm$ decay rates. However, it can be detected as a difference in the $\tau^\pm$ decay angular distributions and is accessible without requiring information about the τ polarization or the determination of the τ rest frame. Limits for the CPV parameter in this decay mode have been published previously by the CLEO Collaboration from an analysis of 13.3 fb^{-1} of data [9].

In the SM, the differential decay width in the hadronic rest frame ($\vec{q}_1 + \vec{q}_2 = 0$) is given by (see [8] for details)

$$d\Gamma_{\tau^-} = \frac{G_F^2}{2m_\tau}\sin^2\theta_c \frac{1}{(4\pi)^3}\frac{(m_\tau^2 - Q^2)^2}{m_\tau^2}|\vec{q}_1| \times \frac{1}{2}\left(\sum_X \bar{L}_X W_X\right)\frac{dQ^2}{\sqrt{Q^2}}\frac{d\cos\theta}{2}\frac{d\alpha}{2\pi}\frac{d\cos\beta}{2}, \quad (1)$$

where G_F is the Fermi coupling constant, θ_c is the Cabibbo angle, m_τ is the mass of the τ lepton, $\vec{q}_1$ and $\vec{q}_2$ denote the three-momenta of the K_S^0 and π^-, respectively, and $Q^2 = (q_1 + q_2)^2$ is the square of the invariant mass of the $K_S^0\pi^\pm$ system. The four hadronic functions W_X with $X \in (B, SA, SF, SG)$ (see [10]) are formed from the vector and scalar form factors $F(Q^2)$ and $F_S(Q^2)$ and are proportional to $|F|^2$, $|F_S|^2$, $\mathrm{Re}(FF_S)$, and $\mathrm{Im}(FF_S)$, respectively. The L_X functions, which contain the angular dependence, can be calculated from electroweak theory (see [8]). The angle β is defined by $\cos\beta = \vec{n}_L \cdot \hat{q}_1$, where $\hat{q}_1 = \vec{q}_1/|\vec{q}_1|$ is the direction of the K_S^0 and $\vec{n}_L$ is the direction of the e^+e^- center of mass (c.m.) system, both observed in the hadronic rest frame. The azimuthal angle α is not observable in this experiment and has to be integrated over. The variable θ is the angle between the direction opposite to the direction of the c.m. system and the direction of the hadronic system in the τ rest frame. In this experiment, the direction of the τ is not known, but θ can be calculated from the hadronic energy E_h measured in the c.m. system:

$$\cos\theta = \frac{2xm_\tau^2 - m_\tau^2 - Q^2}{(m_\tau^2 - Q^2)\sqrt{1 - 4m_\tau^2/s}}, \qquad x = 2\frac{E_h}{\sqrt{s}}, \quad (2)$$

where $s = 4E_{\mathrm{beam}}^2$ denotes the squared c.m. energy.

The effect of the exchange of a charged scalar boson can be introduced by replacing the scalar form factor F_S with

$$F_S(Q^2) \to \tilde{F}_S(Q^2) = F_S(Q^2) + \frac{\eta_S}{m_\tau} F_H(Q^2), \qquad (3)$$

where F_H denotes the form factor for the scalar boson exchange [$F_H = \langle K^0(q_1)\pi^-(q_2)|\bar{u}s|0\rangle$] and η_S is the corresponding dimensionless complex coupling constant [8,11,12]. The differential decay width for the CP conjugate process, $d\Gamma_{\tau^+}$, is obtained from Eqs. (1) and (3) by the replacement $\eta_S \to \eta_S^*$. Using this relation the CP violating quantity is given by [8]

$$\begin{aligned}\Delta_{LW} &\equiv \frac{1}{2}\Big[\sum_X \bar{L}_X W_X(\eta_S) - \sum_X \bar{L}_X W_X(\eta_S^*)\Big]\\ &= -4\frac{m_\tau}{\sqrt{Q^2}}|\vec{q}_1|\mathrm{Im}(FF_H^*)\,\mathrm{Im}(\eta_S)\cos\psi\cos\beta, \qquad (4)\end{aligned}$$

where ψ denotes the angle between the direction of the c.m. frame and the direction of the τ as seen from the hadronic rest frame and can be calculated as

$$\cos\psi = \frac{x(m_\tau^2 + Q^2) - 2Q^2}{(m_\tau^2 - Q^2)\sqrt{x^2 - 4Q^2/s}}. \qquad (5)$$

Since the CP violating term is proportional to $\cos\beta\cos\psi$, it cancels out if one integrates over the angles β and ψ, e.g., for branching fractions. Furthermore, the CP violating effect is only observable if $\mathrm{Im}(FF_H^*) \neq 0$. The form factor F_H is related to the SM weak scalar form factor F_S via

$$F_H(Q^2) = \frac{Q^2}{m_u - m_s} F_S(Q^2), \qquad (6)$$

where m_u and m_s denote the up and strange quark masses, respectively. The derivation of Eq. (6) is discussed in [8] although F_H is not used there explicitly. The chosen value $(m_u - m_s) = -0.1$ GeV$/c^2$ defines the scale of the CPV parameter $\mathrm{Im}(\eta_S)$. Because the CLEO Collaboration used a different relation $F_H = MF_S$ with $M = 1$ GeV$/c^2$ as well as a different normalization of $F_S(Q^2)$, $\mathrm{Im}(\eta_S)$ is not the same as the CP parameter Λ that was used in [9]. In the following, the approximate relation $\mathrm{Im}(\eta_S) \simeq -1.1\Lambda$ is used to enable a comparison of the results.

To extract the CP violating term in Eq. (4), we define an asymmetry in bin i of Q^2 using the difference of the differential τ^+ and τ^- decay widths weighted by $\cos\beta\cos\psi$:

$$\begin{aligned}A_i^{CP} &= \frac{\iint_{Q_{1,i}^2}^{Q_{2,i}^2} \cos\beta\cos\psi\left(\frac{d\Gamma_{\tau^-}}{d\omega} - \frac{d\Gamma_{\tau^+}}{d\omega}\right)d\omega}{\frac{1}{2}\iint_{Q_{1,i}^2}^{Q_{2,i}^2}\left(\frac{d\Gamma_{\tau^-}}{d\omega} + \frac{d\Gamma_{\tau^+}}{d\omega}\right)d\omega}\\ &\simeq \langle\cos\beta\cos\psi\rangle_{\tau^-}^i - \langle\cos\beta\cos\psi\rangle_{\tau^+}^i, \qquad (7)\end{aligned}$$

with $d\omega = dQ^2 d\cos\theta d\cos\beta$. In other words, A^{CP} is the difference between the mean values of $\cos\beta\cos\psi$ for τ^+ and τ^- events evaluated in bins of Q^2.

We use 699 fb^{-1} of data collected at the $\Upsilon(3S)$, $\Upsilon(4S)$, and $\Upsilon(5S)$ resonances and off resonance with the Belle detector [13] at the KEKB asymmetric-energy e^+e^- collider [14]. The signal and backgrounds from $\tau^+\tau^-$ events are generated by KKMC/TAUOLA [15]. The detector response is simulated by a GEANT3 [16] based program.

Using standard event topology requirements, a $e^+e^- \to \tau^+\tau^-(\gamma)$ sample is selected as described in [17].

In the c.m. frame, the event is divided into two hemispheres using the plane perpendicular to the direction of the thrust axis [18]. Events with one charged track from an electron, muon, or pion in one hemisphere (tag side) and a charged pion and a $K_S^0 \to \pi^+\pi^-$ candidate in the other hemisphere (signal side) are chosen. The K_S^0 candidates are required to have an invariant mass in the range $0.485 < M_{\pi\pi} < 0.511$ GeV$/c^2$ and a reconstructed K_S^0 decay length greater than 2 cm. The selection criteria for the signal side and particle identification criteria are described in detail in [19]. Backgrounds from decays with a π^0 are suppressed by rejecting events containing photons on the signal side with energies greater than 0.15 GeV. To further suppress background from $e^+e^- \to q\bar{q}$ ($q = u, d, s$, and c) processes, a thrust value above 0.9 is required, and for events with a pion on the tag side, the number of tag side photons with energies greater than 0.1 GeV must be less than five. In total, $(162.2 \pm 0.4) \times 10^3$ $\tau^+ \to K_S^0\pi^+\bar{\nu}_\tau$ and $(162.0 \pm 0.4) \times 10^3$ $\tau^- \to K_S^0\pi^-\nu_\tau$ candidates are selected. Background contributions from τ decays with the exception of $\tau^\pm \to \nu_\tau\pi^\pm\pi^+\pi^-$ and contributions from $e^+e^- \to q\bar{q}$ and two-photon processes are estimated from Monte Carlo (MC) simulation [20–22] using the branching fractions from [23]. Contributions from $\tau^\pm \to \nu_\tau\pi^\pm\pi^+\pi^-$ are estimated using the data in the two K_S^0 sideband regions, $0.469 < M_{\pi\pi} < 0.482$ GeV$/c^2$ and $0.514 < M_{\pi\pi} < 0.527$ GeV$/c^2$ [24].

The largest background contribution is due to other τ decays, namely, $(9.5 \pm 3.2)\%$ of the events in the selected signal sample from $\tau^\pm \to \nu_\tau K_S^0 K_L^0\pi^\pm$, $(3.7 \pm 1.2)\%$ from $\tau^\pm \to \nu_\tau K_S^0\pi^\pm\pi^0$, $(1.7 \pm 0.2)\%$ from $\tau^\pm \to \nu_\tau K_S^0 K^\pm$, and $(1.79 \pm 0.03)\%$ from $\tau^\pm \to \nu_\tau\pi^\pm\pi^+\pi^-$. The contribution from $e^+e^- \to q\bar{q}$ is $(3.4 \pm 1.0)\%$. The backgrounds from $b\bar{b}$, Bhabha, and two-photon processes are negligible. The total contribution of background processes is $(22.1 \pm 3.6)\%$. The invariant mass of the $K_S^0\pi^\pm$ system, $W = \sqrt{Q^2}$, for the selected data events is shown in Fig. 1 together with simulated signal events and the background contributions discussed above. Signal events were generated by a modified version of TAUOLA that incorporates the results of [19].

To avoid possible bias, the CPV search is performed as a blind analysis. First, possible sources of artificial CPV, such as forward-backward (FB) asymmetries in the $e^+e^- \to \tau^+\tau^-$ production ($\gamma - Z$ interference effects and higher-order QED effects) and detector induced differences between π^+ and π^- reconstruction efficiencies, are studied using the data. Other unknown sources are

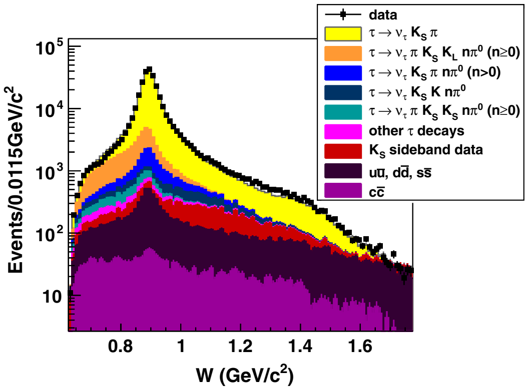

FIG. 1 (color online). Mass spectrum of the $K_S^0\pi^\pm$ system. Data are indicated by the squares, simulated signal and the estimated background contributions are shown by the colored histograms. All background modes have been determined from Monte Carlo simulations with the exception of $\tau^\pm \to \nu_\tau\pi^\pm\pi^+\pi^-$ which has been estimated from K_S^0 sideband data.

investigated in the data by measuring the CP asymmetry in a control sample described below.

The FB asymmetry is measured in $\tau^\pm \to \nu_\tau\pi^\pm\pi^+\pi^-$ events (excluding $K_S^0 \to \pi^+\pi^-$ signal candidates by using a mass and decay length veto) as a function of the momentum and polar angle of the $\pi^\pm\pi^+\pi^-$ system. An effect of a few percent is observed, which is described well by the MC simulation. The asymmetry for $\pi^\pm$ detection, which can arise because of the different nuclear interaction cross sections for positively and negatively charged hadrons, is studied in the laboratory system as a function of momentum and polar angle of the charged pions in $\tau^\pm \to \nu_\tau\pi^\pm\pi^+\pi^-$ (excluding $\pi^+\pi^-$ combinations consistent with K_S^0 decays) events and found to be of $O(10^{-2})$ (see [25] for details). Using these measurements, correction tables are obtained that are then applied as weights for each event. Since the CP asymmetry is measured as a function of angles relative to the τ direction rather than polar angles in the laboratory, the net effect of these corrections on the CP asymmetry is very small [$O(10^{-4})$ for FB asymmetry effects and $O(10^{-3})$ for the $\pi^\pm$ detection asymmetry].

A control sample is selected from $\tau^\pm \to \nu_\tau\pi^\pm\pi^+\pi^-$ events [26] by requiring that the invariant mass of both $\pi^+\pi^-$ combinations lie outside of the K_S^0 mass window but the mass of one of the combinations lie in the sideband of this window. The resulting sample consists of about 10^6 events, i.e., about 3 times more than the signal sample. The CP asymmetry measured in this control sample is very small [$O(10^{-3})$] (see [25] for details) and serves as an estimate of the remaining unknown systematic effects.

The observed CP asymmetry in the selected $\tau^\pm \to K_S^0\pi^\pm\nu_\tau$ candidate sample is shown in Table I for four bins of the hadronic mass $W = \sqrt{Q^2}$ before and after applying the corrections for higher-order QED and $\pi^\pm$ detection asymmetry effects. The fourth column shows the final values of the CP asymmetry after subtraction of the background contributions. Here, we assume that there is no CP asymmetry in the background and correct the background effects as

$$A_i^{CP} = \frac{\langle\cos\beta\cos\psi\rangle^i_{\tau^-}}{1 - f^-_{b,i}} - \frac{\langle\cos\beta\cos\psi\rangle^i_{\tau^+}}{1 - f^+_{b,i}}, \qquad (8)$$

where $f^\pm_{b,i}$ are the fractions of background in the selected $\tau^\pm$ samples in W bin i.

In order to account for possible systematic uncertainties due to detector effects, the quadratic sum of the values of A^{CP} measured in the control sample and their statistical errors are used as an estimate of the systematic error. Other contributions to the systematic error arise in the background subtraction because of uncertainties in the estimated number of background candidates and limited MC statistics. These contributions are, however, small in comparison. A summary of the systematic uncertainties is given in Table II.

The background subtracted asymmetry is shown in Figs. 2(a) and 2(b) with statistical and systematic errors added in quadrature. The asymmetry is small and except for the lowest mass bin within 1 standard deviation (σ) of zero. For comparison, the predicted CP asymmetry is shown in Fig. 2(a) for $\mathrm{Im}(\eta_S) = 0.1$ and $\mathrm{Re}(\eta_S) = 0$ [27]. Note that the current best limit by the CLEO experiment [9] corresponds to $|\mathrm{Im}(\eta_S)| < 0.19$.

TABLE I. CP asymmetry A^{CP} measured in bins of the hadronic mass W. The second and third columns show the observed asymmetry with statistical errors only, before and after correcting for higher-order QED and $\pi^\pm$ detection asymmetry effects. The final CP asymmetry after background subtraction is shown in the fourth column where first and second errors correspond to statistical and systematic errors, respectively. The fifth column shows the observed number of signal events n_i per W bin (after background subtraction) divided by $N_s = \sum_i n_i$.

W (GeV/c^2)	Observed	A^{CP} (10^{-3}) Corrected	Backgr. subtr.	n_i/N_s (%)
0.625–0.890	-0.1 ± 2.1	5.2 ± 2.1	$7.9 \pm 3.0 \pm 2.8$	36.53 ± 0.14
0.890–1.110	-2.7 ± 1.7	1.6 ± 1.7	$1.8 \pm 2.1 \pm 1.4$	57.85 ± 0.15
1.110–1.420	-5.1 ± 4.7	-3.5 ± 4.7	$-4.6 \pm 7.2 \pm 1.7$	4.87 ± 0.04
1.420–1.775	9.3 ± 12.1	9.6 ± 12.1	$-2.3 \pm 19.1 \pm 5.5$	0.75 ± 0.02

TABLE II. Systematic uncertainties in the CP asymmetry A^{CP}. The second column shows the uncertainties due to effects introduced by the detector, which are estimated from the A^{CP} measurement in the control sample. Contributions from uncertainties in the background estimates and limited MC statistics are small in comparison.

	Systematic uncertainties (10^{-3})			
W (GeV/c^2)	Detector	Backgr.	MC stat.	Total
0.625–0.890	2.76	0.59	0.15	2.83
0.890–1.110	1.40	0.04	0.10	1.40
1.110–1.420	1.50	0.25	0.79	1.71
1.420–1.775	5.18	0.96	1.38	5.45

From the measured values of A^{CP} the CPV parameter $\mathrm{Im}(\eta_S)$ can be extracted, which allows an interpretation in the context of NP models. Taking into account the detector efficiencies, the relation between A^{CP} and $\mathrm{Im}(\eta_S)$ is given as

$$A_i^{CP} \simeq \mathrm{Im}(\eta_S)\frac{N_s}{n_i}\int_{Q^2_{1,i}}^{Q^2_{2,i}} C(Q^2)\frac{\mathrm{Im}(FF_H^*)}{m_\tau}dQ^2 \equiv c_i\,\mathrm{Im}(\eta_S), \tag{9}$$

where n_i is the observed number of $\tau^\pm \to K_S^0\pi^\pm\nu_\tau$ events in Q^2 bin i ($Q^2 \in [Q^2_{1,i}, Q^2_{2,i}]$) and $N_s = \sum_i n_i$ is the total number of observed $\tau^\pm \to K_S^0\pi^\pm\nu_\tau$ events. The function $C(Q^2)$ includes the detector efficiency as well as all model-independent terms. First, the efficiency is determined as a function of Q^2, β, and θ, then $C(Q^2)$ is obtained after numerical integration over the decay angles β and θ. The parametrization of $C(Q^2)$ is given in [25].

Using the function $C(Q^2)$ and the fractions N_s/n_i which are given in Table I, the linearity constants c_i, which relate A^{CP} and $\mathrm{Im}(\eta_S)$, can be determined for any parametrization of the form factors F and F_H simply by calculating the integral in Eq. (9) [28].

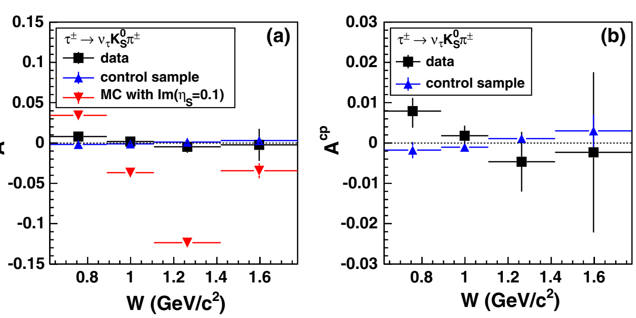

FIG. 2 (color online). (a) Measured CP violation asymmetry after background subtraction (squares). The vertical error bars are the statistical error and systematic errors added in quadrature. The CP asymmetry measured in the control sample is indicated by the blue triangles (statistical errors only) and the inverted red triangles show the expected asymmetry for $\mathrm{Im}(\eta_S) = 0.1$ [$\mathrm{Re}(\eta_S) = 0$]. (b) Expanded view (the vertical scale is reduced by a factor of 5).

To determine limits for $|\mathrm{Im}(\eta_S)|$, three parametrizations of F and F_S [exploiting Eq. (6)] as linear combinations of Breit-Wigner shapes of the vector resonances $K^*(892)$ and $K^*(1410)$ and the scalar resonances $K_0^*(800)$ and $K_0^*(1430)$ are used. These parametrizations were determined in an earlier Belle measurement of the $K_S^0\pi^\pm$ mass spectrum [19]. In addition, a constant strong interaction phase difference between F and F_S, $\phi_S = \arg[F_S(Q^2_{\min})] - \arg[F(Q^2_{\min})]$ with $Q^2_{\min} = (m_\pi + m_{K_S^0})^2$, is introduced for generality because such a relative phase cannot be determined from the $K_S^0\pi^\pm$ mass spectrum.

Using Eq. (9), the linearity constants c_i are calculated in each mass bin for $\phi_S = 0°, 5°, \ldots, 360°$ and the obtained values of $\mathrm{Im}(\eta_S)$ with associated uncertainties are combined to determine upper limits for $|\mathrm{Im}(\eta_S)|$. For each parametrization, the value ϕ_S giving the most conservative limit is chosen. For the three parametrizations of F and F_S, this results in the range of limits $|\mathrm{Im}(\eta_S)| < (0.012\text{–}0.026)$ at 90% confidence level. If we fix $\phi_S \equiv 0$, the range $|\mathrm{Im}(\eta_S)| < (0.011\text{–}0.023)$ is obtained. The parametrizations of F and F_S used by the CLEO Collaboration [9] yield a comparable limit $|\mathrm{Im}(\eta_S)| < 0.013$. These results are about 1 order of magnitude more restrictive than the previous best upper limit, $|\mathrm{Im}(\eta_S)| < 0.19$, obtained by the CLEO Collaboration [9].

Theoretical predictions for $\mathrm{Im}(\eta_S)$ can be given in the context of a MHDM with three or more Higgs doublets [4,5]. In such models η_S is given by [12]

$$\eta_S \simeq \frac{m_\tau m_s}{M^2_{H^\pm}}X^*Z \tag{10}$$

if numerically small terms proportional to m_u are ignored. Here, $M_{H^\pm}$ is the mass of the lightest charged Higgs boson and the complex constants Z and X describe the coupling of the Higgs boson to the τ and ν_τ and the u and s quarks, respectively (see [5,12]). The limit $|\mathrm{Im}(\eta_S)| < 0.026$ is therefore equivalent to

$$|\mathrm{Im}(XZ^*)| < 0.15\frac{M^2_{H^\pm}}{1\ \mathrm{GeV}^2/c^4}. \tag{11}$$

In summary, we have searched for CP violation in $\tau^\pm \to K_S^0\pi^\pm\nu_\tau$ decays, analyzing the decay angular distributions. No significant CP asymmetry has been observed. Upper limits for the CP violation parameter $\mathrm{Im}(\eta_S)$ at 90% confidence level are in the range $|\mathrm{Im}(\eta_S)| < 0.026$ or better, depending on the parametrization used to describe the hadronic form factors and improve upon previous limits by 1 order of magnitude.

We acknowledge J. H. Kühn, K. Kiers, and T. Morozumi for useful discussions. We thank the KEKB group for excellent operation of the accelerator, the KEK cryogenics group for efficient solenoid operations, and the KEK computer group and the NII for valuable computing and SINET4 network support. We acknowledge support from MEXT, JSPS, and Nagoya's TLPRC (Japan); ARC and

DIISR (Australia); NSFC (China); MSMT (Czechia); DST (India); MEST, NRF, NSDC of KISTI, and WCU (Korea); MNiSW (Poland); MES and RFAAE (Russia); ARRS (Slovenia); SNSF (Switzerland); NSC and MOE (Taiwan); and DOE (U.S.).

[1] M. Kobayashi and T. Maskawa, Prog. Theor. Phys. **49**, 652 (1973).
[2] E. Christova, H. Eberl, W. Majerotto, and S. Kraml, J. High Energy Phys. 12 (2002) 021.
[3] T. Ibrahim and P. Nath, Rev. Mod. Phys. **80**, 577 (2008).
[4] S. Weinberg, Phys. Rev. Lett. **37**, 657 (1976).
[5] Y. Grossman, Nucl. Phys. **B426**, 355 (1994).
[6] I. I. Bigi and A. I. Sanda, Phys. Lett. B **625**, 47 (2005).
[7] G. Calderon, D. Delepine, and G. Lopez Castro, Phys. Rev. D **75**, 076001 (2007).
[8] J. H. Kühn and E. Mirkes, Phys. Lett. B **398**, 407 (1997).
[9] G. Bonvicini *et al.* (CLEO Collaboration), Phys. Rev. Lett. **88**, 111803 (2002).
[10] J. H. Kühn and E. Mirkes, Z. Phys. C **56**, 661 (1992).
[11] K. Kiers *et al.*, Phys. Rev. D **78**, 113008 (2008).
[12] S. Y. Choi, K. Hagiwara, and M. Tanabashi, Phys. Rev. D **52**, 1614 (1995).
[13] A. Abashian *et al.*, Nucl. Instrum. Methods Phys. Res., Sect. A **479**, 117 (2002).
[14] S. Kurokawa *et al.*, Nucl. Instrum. Methods Phys. Res., Sect. A **499**, 1 (2003), and other papers included in this volume.
[15] S. Jadach, B. F. L. Ward, and Z. Was, Comput. Phys. Commun. **130**, 260 (2000).
[16] R. Brun, F. Bruyant, M. Maire, A. C. McPherson, and P. Zanarini, CERN Report No. DD/EE/84-1, 1984.
[17] M. Fujikawa *et al.* (Belle Collaboration), Phys. Rev. D **78**, 072006 (2008).
[18] E. Farhi, Phys. Rev. Lett. **39**, 1587 (1977).
[19] D. Epifanov *et al.* (Belle Collaboration), Phys. Lett. B **654**, 65 (2007).
[20] D. J. Lange, Nucl. Instrum. Methods Phys. Res., Sect. A **462**, 152 (2001).
[21] S. Jadach, E. Richter-Was, B. F. L. Ward, and Z. Was, Comput. Phys. Commun. **70**, 305 (1992).
[22] F. A. Berends, P. H. Daverveldt, and R. Kleiss, Comput. Phys. Commun. **40**, 285 (1986).
[23] K. Nakamura *et al.* (Particle Data Group), J. Phys. G **37**, 075021 (2010).
[24] The contributions of the simulated background modes were subtracted from the data in K_S^0 sideband regions in order to avoid double counting.
[25] See supplemental material at http://link.aps.org/supplemental/10.1103/PhysRevLett.107.131801 for details on the corrections of the experimental asymmetries, the measured CP asymmetry in the control sample, and the derivation of the function $C(Q^2)$.
[26] Possible CP violation in this decay mode is expected to be small because of the small Higgs coupling to the d quark and is smeared out only if the two-body decay angle β (and ψ) is measured (see [9]).
[27] The prediction is obtained from MC simulations by using solution 1 of Table 4 in [15] as parametrizations for the form factors F and F_S together with Eq. (6).
[28] This allows for a simple reevaluation of limits for $\mathrm{Im}(\eta_S)$ when better knowledge for the form factors is available from theory or future measurements.